ChemComm

Chemical Communications

rsc.li/chemcomm

ROYAL SOCIETY
OF **CHEMISTRY**

COMMUNICATION
Yukiko Kamiya, Hiroyuki Asanuma *et al.*
Unexpectedly stable homopurine parallel triplex of
SNA:RNA*SNA and L-*a*TNA:RNA*L-*a*TNA

60 YEARS
ANNIVERSARY

COMMUNICATION

Check for updates

Unexpectedly stable homopurine parallel triplex of SNA:RNA*SNA and L-*a*TNA:RNA*L-*a*TNA†

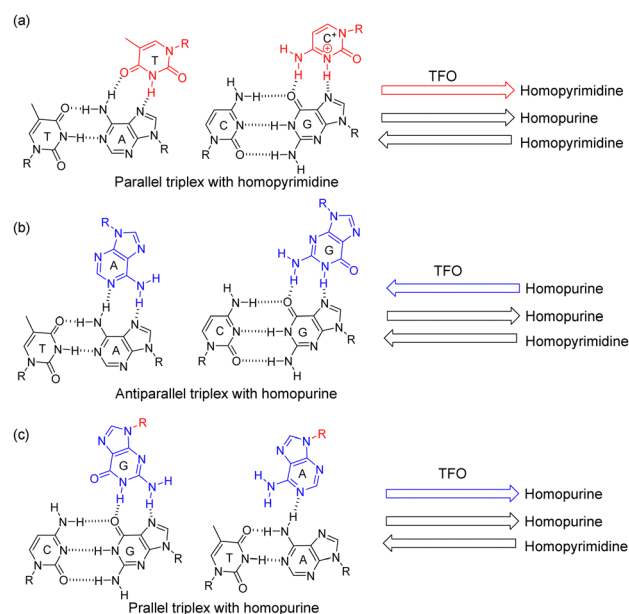Yukiko Kamiya, [iD] *[abc] Siyuan Lao,[a] Jumpei Ariyoshi,[b] Fuminori Sato[a] and Hiroyuki Asanuma [iD] *[a]

Homopurine strands are known to form antiparallel triplexes stabilized by G*G and A*A Hoogsteen pairs, which have two hydrogen bonds. But there has been no report on the parallel triplex formation of homopurine involving both adenosine and guanosine to the duplex. In this paper, we first report parallel triplex formation between a homopurine serinol nucleic acid (SNA) strand and an RNA/SNA duplex. Melting profiles revealed that the parallel SNA:RNA*SNA triplex was remarkably stable, even though the A*A pair has a single hydrogen bond. An L-acyclic threoninol nucleic acid (L-*a*TNA) homopurine strand also formed a stable parallel triplex with an L-*a*TNA/RNA duplex.

Non-canonical base-pairing enables formation of multistranded nucleic acid structures such as triplexes,[1–6] G-quadruplexes,[7–10] and i-motifs.[11,12] Parallel triplexes form under slightly acidic conditions when a homopyrimidine strand recognizes a Watson–Crick duplex through Hoogsteen pairing.[4–6] Antiparallel triplexes with the third strand composed of only thymidine or homopurine have also been characterised.[13,14] Non-natural nucleobases and xeno nucleic acids (XNAs) with non-ribose scaffolds also form multi-stranded structures. Homo-adenine is reported to form triplex mediated by cyanuric acid.[15] Two peptide nucleic acids (PNAs) with homopyrimidines bind single-stranded homopurine DNA to form a parallel triplex.[16,17] Tight binding of PNAs enables strand-invasive recognition of DNA duplex. Our group has synthesized and characterized the duplex formed by serinol nucleic acid (SNA)[18] and acyclic threoninol nucleic acid (*a*TNA) with either D- or L-threoninol as a scaffold.[19,20] L-*a*TNA with

a homopyrimidine sequence is reported to form parallel triplex with DNA similar to PNA.[21]

Thymidine- and cytidine-containing oligonucleotides form parallel triplexes but homothymidine triplex-forming oligonucleotide (TFO) may also form parallel or antiparallel triplexes (Scheme 1a).[4–6,13,14] However, homopurine strands involving both guanosine and adenosine have only been reported to form antiparallel triplexes (Scheme 1b).[13,14] This may be because if the TFO involves adenine taking anti conformation, only a single hydrogen bond is possible with the duplex (Scheme 1c).[14] Furthermore, as the sequences of the duplex-forming homopurine strand and the TFO are the same, analysis of the triplex is difficult.

Recently, our group has successfully resolved the crystal structures of L-*a*TNA:RNA and SNA:RNA heteroduplexes.[22] We

Scheme 1 Hydrogen bonds formed by triplex structures with (a) a parallel homopyrimidine TFO, (b) an antiparallel homopurine TFO, and (c) a parallel homopurine TFO.

[a] *Department of Biomolecular Engineering, Graduate School of Engineering, Nagoya University, Furo-cho, Chikusa-ku, Nagoya 464-8603, Japan. E-mail: asanuma@chembio.nagoya-u.ac.jp*
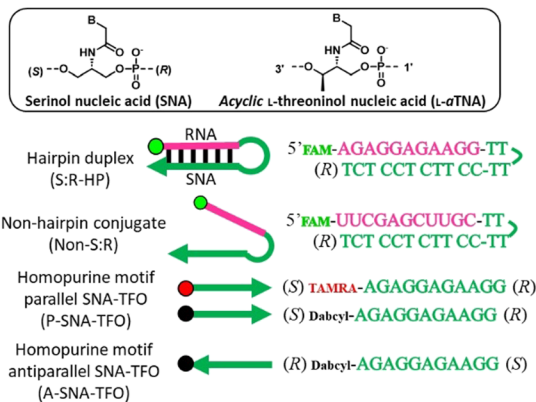
[b] *Laboratory of Bioanalytical Chemistry, Kobe Pharmaceutical University, Higashinada-Ku, Kobe, 658-8558, Japan. E-mail: y-kamiya@kobepharma.ac.jp*

[c] *Institute for Molecular Science, National Institutes of Natural Sciences, Okazaki, Aichi 444-8585, Japan*

† Electronic supplementary information (ESI) available. See DOI: https://doi.org/10.1039/d3cc05555h
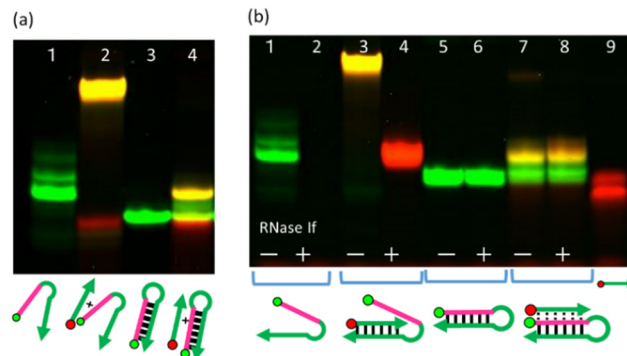
Scheme 2 Chemical structures of SNA and L-aTNA, and schematics and sequences of select oligonucleotides used in this study. For all oligo-nucleotide sequences, see Scheme S2 (ESI†).

Fig. 1 PAGE analyses of (a) FAM-Non-S:R only (lane 1); FAM-Non-S:R + TAMRA-P-SNA-TFO (lane 2); FAM-S:R-HP only (lane 3); FAM-S:R-HP + TAMRA-P-SNA-TFO (lane 4) and of (b) FAM-Non-S:R only without (lane 1) and with (lane 2) RNase If; FAM-Non-S:R + TAMRA-P-SNA-TFO without (lane 3) and with (lane 4) RNase If; FAM-S:R-HP only without (lane 5) and with (lane 6) RNase If; FAM-S:R-HP + TAMRA-P-SNA-TFO without (lane 7) and with (lane 8) RNase If; and TAMRA-P-SNA-TFO only without RNase If (lane 9). 0.5 μM each oligonucleotide was used.

found that both heteroduplexes were unwound relative to the RNA helical structure and that base pairs aligned perpendicularly to the helical axis, different from canonical B- or A-type duplexes. Interestingly and unexpectedly, in the crystals, we observed triplex structures at the termini of both heteroduplexes (Fig. S1, ESI†). These triplex structures involved C:G*G Watson–Crick and Hoogsteen pairs with RNA in a parallel orientation. This result prompted us to study XNA:RNA*XNA triplexes with the homopurine XNA TFO in the parallel orientation.

To examine parallel triplex formation of SNA-TFO, we used an RNA–SNA oligonucleotide that forms a hairpin (S:R-HP) as a template to avoid formation of an SNA:SNA duplex (Scheme 2 and S2, ESI†), and a TFO designed to bind to S:R-HP in parallel fashion (P-SNA-TFO). The use of a hairpin was necessary because an SNA:SNA duplex is more stable than an SNA:RNA duplex,[23,24] and unless a hairpin is used, strand invasion would lead to an SNA:SNA duplex rather than a triplex. The melting temperature (T_m) of the S:R-HP was 80.5 °C (Fig. S2, ESI†). An RNA–SNA oligonucleotide that cannot form a hairpin in which only the SNA region is complementary to P-SNA-TFO was used as a negative control (Non-S:R, Scheme 2). S:R-HP and Non-S:R were labelled at the 5′ termini with FAM (green); TAMRA (red) was conjugated to the (S) terminus of P-SNA-TFO. Note that the G-rich TFO might form anti-parallel G-quadruplexes (Fig. S3, ESI†).[25]

We analysed triplex formation by native polyacrylamide electrophoresis (PAGE). When P-SNA-TFO was mixed with Non-S:R, which should result in formation of a duplex, a yellow band with overlapping green and red bands was observed that migrated more slowly than Non-S:R (Fig. 1a, lanes 1 and 2). Mixing of S:R-HP and P-SNA-TFO also resulted in a yellow band that migrated more slowly than S:R-HP (Fig. 1a, lanes 3 and 4), but the position was different from that of the P-SNA-TFO:Non-S:R duplex. To rule out the possibility that strand invasion had resulted in a P-SNA-TFO:SNA duplex, we incubated samples with RNase If, which selectively digests single-stranded RNA.[26]
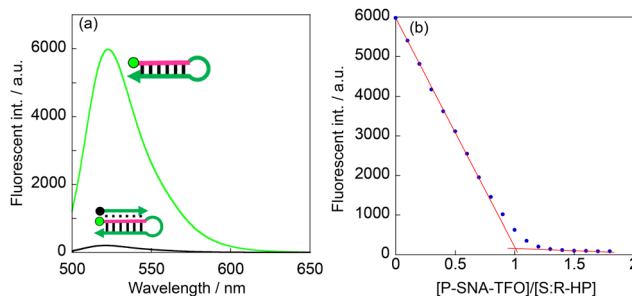
If a P-SNA-TFO:SNA duplex was formed, the single-stranded RNA should be digested by RNase If. Neither S:R-HP nor S:R-HP in the complex with P-SNA-TFO were digested by RNase If (Fig. 1b, lanes 5–8), whereas both Non-S:R and Non-S:R in the
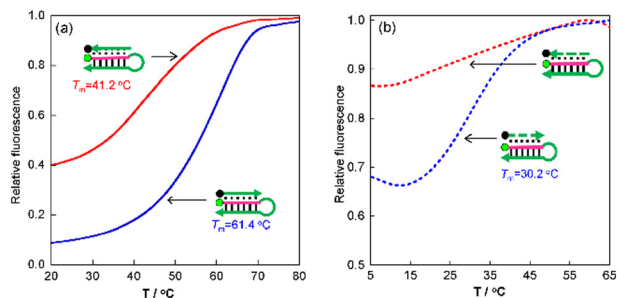
complex with P-SNA-TFO were completely digested (Fig. 1b, lanes 1–4), clearly demonstrating that a triplex was formed by P-SNA-TFO and the S:R-HP.

Next, we examined stoichiometries and T_ms of complexes by replacing the TAMRA on the (S) terminus of the P-SNA-TFO with quencher Dabcyl (Scheme 2). When FAM-S:R-HP was mixed with Dabcyl-P-SNA-TFO, FAM fluorescence was considerably quenched (Fig. 2a). Fluorescent titration revealed that triplex formation proceeded via 1:1 complexation of the S:R-HP and P-SNA-TFO (Fig. 2b). From the melting profile of FAM fluorescence, the T_m of the parallel triplex was 61.4 °C (Fig. 3, blue line), which was higher than the T_m of the antiparallel triplex (41.2 °C, Fig. 3, red line). It should be noted that A*A pair in parallel triplex has only single hydrogen bond (Scheme 1c), whereas it has two in the antiparallel triplex. Despite this, the T_m of the parallel SNA:RNA*SNA triplex was considerably higher than those of the antiparallel triplexes. Although homopurine TFO could form both parallel and antiparallel triplexes,

Fig. 2 (a) Fluorescence of FAM conjugated to S:R-HP in the presence and absence of Dabcyl-P-SNA-TFO. [S:R-HP] = 1.79 μM, [P-SNA-TFO] = 2.14 μM. 90 mM Tris-borate buffer, 10 mM MgCl₂, pH 7.0, 4 °C. (b) Fluorescence of FAM-S:R-HP as a function of the ratio of [Dabcyl-P-SNA-TFO] to [S:R-HP]. Initial [S:R-HP] = 2.0 μM, 90 mM Tris-borate buffer, 10 mM MgCl₂, pH 7.0, 4 °C. Excitation wavelength was 495 nm, and fluorescence intensity was monitored at 523 nm. See ESI† for the titration experiment.

Fig. 3 Melting profiles of FAM-S:R-HP with (a) homopurine-motif TFO: P-SNA-TFO (blue line) and A-SNA-TFO (red line) and (b) homopyrimidine-motif-TFO: Y-P-SNA-TFO (blue dotted line), and Y-A-SNA-TFO (red dotted line). 2.0 μM each oligonucleotide solved in 90 mM Tris-borate buffer, 10 mM MgCl$_2$, pH 7.0 was used. Excitation wavelength was 495 nm, and fluorescence intensity was monitored at 523 nm.
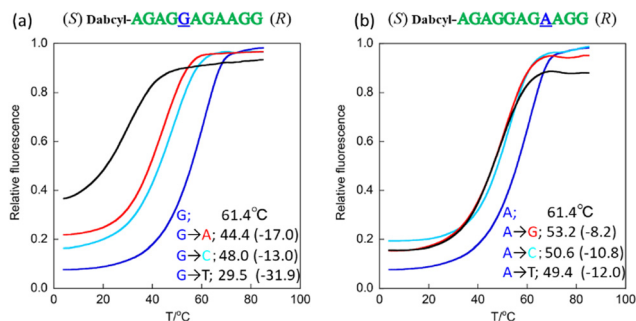
they may have different base-stacking geometries. Additionally, we compared T_m of the homopurine triplex to that of the homopyrimidine triplex (Scheme S2, ESI†). As expected from the previous report,[21] homopyrimidine TFO formed parallel triplex (Fig. 3b), but less stable than the homopurine parallel triplex (Fig. 3a). The homopyrimidine TFO did not form anti-parallel type triplex (Fig. 3b).

We next examined whether L-*a*TNA can form a parallel triplex with an RNA-L-*a*TNA hairpin (LT:R-HP, Scheme S2, ESI†). As observed in fluorescence experiments with the SNA-based system, fluorescence of FAM-LT:R-HP was considerably quenched in the presence of Dabcyl-P-L-*a*TNA-TFO, and the fluorescence titration showed that a 1:1 complex was formed (Fig. S4a, ESI†). The T_m of the triplex formed with the L-*a*TNA-TFO was 74.2 °C (Fig. S4b, ESI†), 13 °C higher than the T_m of the parallel SNA triplex. We also confirmed that homopyrimidine L-*a*TNA-TFO did not form antiparallel triplex but parallel triplex (Fig. S4c, ESI†). These results indicate that scaffold structures of SNA and L-*a*TNA result in stable parallel triplexes containing a single RNA strand.
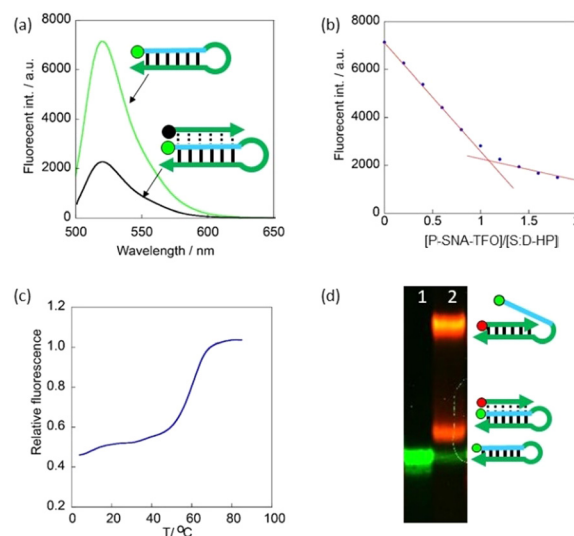
To examine the sequence specificity of parallel triplex formation, we measured T_ms of mismatched SNA-TFOs. When a guanine near the centre of the TFO was replaced with a different nucleobase, the T_m remarkably decreased by 15–30 °C (Fig. 4a). When an adenine near the centre was replaced, the T_m decreased, but the decrease was around 10 °C (Fig. 4b), smaller in magnitude than observed when guanine was substituted. Similar sequence-specificity was also observed for the L-*a*TNA triplex (Fig. S5, ESI†). These results indicate that G*G and A*A pairs stabilize the triplex. The smaller decrease in T_m when adenine was replaced compared to guanine is likely because there is a single hydrogen bond in the A*A pair and two in the G*G pair.

Finally, we investigated triplex formation with DNA in the hairpin. Unlike RNA, quenching of FAM conjugated to S:D-HP by the P-SNA-TFO was inefficient (Fig. 5a). A titration showed an inflection point at a 1:1 ratio of S:D-HP to P-SNA-TFO (Fig. 5b), and a clear sigmoid curve of melting profile was observed (Fig. 5c). The T_m was 59.9 °C, which was comparable to that of RNA-containing parallel triplex (61.4 °C). PAGE analysis revealed the reason for inefficient quenching. In the sample containing FAM-S:D-HP and TAMRA-P-SNA-TFO two yellow bands were observed that were assigned to triplex and invaded duplex (Fig. 5d). Since the SNA:DNA duplex is less stable than the SNA:RNA duplex,[20] some P-SNA-TFO invaded into the hairpin. When the DNA portion of S:D-HP is single stranded, the 5′ FAM is not quenched by the Dabcyl on the P-SNA-TFO. We also examined whether an SNA:SNA*SNA triplex was formed using the same strategy. Little quenching was detected (Fig. S6, ESI†). Thus, we concluded that a parallel triplex is formed only on DNA and RNA.

Fig. 5 (a) Fluorescence of FAM conjugated to S:D-HP in the presence and absence of Dabcyl-P-SNA-TFO. [S:D-HP] = 2.0 μM, [P-SNA-TFO] = 2.4 μM. 90 mM Tris-borate buffer, 10 mM MgCl$_2$, pH 7.0, 4 °C. Excitation wavelength was 495 nm. (b) Fluorescence of FAM-S:D-HP as a function of the ratio of [Dabcyl-P-SNA-TFO] to [S:D-HP]. Initial [S:D-HP] = 2.0 μM, 90 mM Tris-borate buffer, 10 mM MgCl$_2$, pH 7.0, 4 °C. Fluorescence intensity was monitored at 523 nm. (c) Melting profile of S:D-HP and P-SNA-TFO triplex. [P-SNA-TFO] = [S:D-HP] = 2.0 μM. (d) PAGE analysis of FAM-S:D-HP (lane 1) and FAM-S:D-HP + TAMRA-P-SNA-TFO (lane 2). [TAMRA-P-SNA-TFO] = [FAM-S:D-HP] = 0.4 μM.
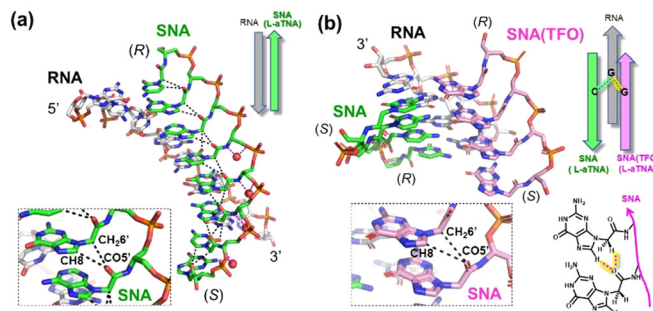

Fig. 4 Melting profiles of triplex of S:R-HP and P-SNA-TFO with (a) guanosine near the centre (underlined in blue in the sequence) or (b) adenosine near the centre (underlined blue in the sequence) replaced with indicated nucleotide. [P-SNA-TFO] = [S:R-HP] = 2.0 μM, 90 mM Tris-borate buffer, 10 mM MgCl$_2$, pH 7.0. Excitation wavelength was 495 nm, and fluorescence intensity was monitored at 523 nm.

Fig. 6 (a) Crystal structure of anti-parallel duplex of SNA and RNA. Hydrogen bonds between C═O and both −CH$_2$− and H8 of purine observed in the crystal structure of the RNA:SNA duplex (PDB: 7bpg). (b) Computer modelling of SNA:RNA*SNA triplex stabilized by hydrogen bonds between the carbonyl and adjacent hydrogens based on the crystal structure. Hydrogen atoms are omitted for clarity.

SNA- and L-*a*TNA-TFOs formed stable parallel triplexes even though an A*A pair has a single hydrogen bond. Previous X-ray crystallographic analyses of SNA:RNA and L-*a*TNA:RNA duplexes revealed unique hydrogen bonds of C═O with −CH$_2$− and H8 of purine to fix the conformation of SNA and L-*a*TNA (Fig. 6a).[22] Computer modelling with these hydrogen bonds suggest that these hydrogen bonds stabilize the parallel triplexes involving an RNA and SNA or L-*a*TNA duplex and an XNA TFO (Fig. 6b). In contrast, the antiparallel conformation does not allow these hydrogen bonds. Thus, the single hydrogen bond in A*A pair is compensated for by these additional hydrogen bonds, which stabilize the parallel triplex.

In conclusion, we discovered that homopurine SNA and L-*a*TNA oligonucleotides form XNA:RNA*XNA and XNA:DNA*XNA parallel triplexes in a sequence-specific manner. Even though the A*A pair has a single hydrogen bonding, the parallel triplex was considerably more stable than the antiparallel triplex in which the A*A pair has two hydrogen bonds. The unexpectedly stable parallel triplex results from the interaction of C═O with both −CH$_2$− and H8 of purine. Note that interior linker that connects nucleobase and main chain is one atom longer for SNA and L-*a*TNA than DNA and PNA, which may give flexibility and allowed both parallel and antiparallel triplex with homopurine TFO. The parallel triplex is thus specific to SNA and L-*a*TNA and is a new supramolecular motif that should prove useful in XNA-based nanotechnology.[27] This is the first example of parallel triplex formation with a homopurine sequence. Unlike conventional homopyrimidine TFO, homopurine TFO does not require acidic conditions. Therefore, parallel homopurine TFO will be able to capture purine-rich RNA in cells under physiological conditions. In order to target single-stranded RNA in cells, formation of SNA or L-*a*TNA homoduplexes must be suppressed. For this purpose, replacement of the A–T pair with a pseudo-complementary 2,6-diaminopurine-thiouracil pair will be effective.[28,29] We have recently succeeded in the incorporation of diaminopurine and thiouracil into SNA and L-*a*TNA.[23,24]

Conflicts of interest

There are no conflicts to declare.

References

1 G. Felsenfeld, D. Davies and A. Rich, *J. Am. Chem. Soc.*, 1957, **79**, 2023.
2 K. Hoogsteen, *Acta Crystallogr.*, 1959, **12**, 822.
3 N. T. Thuong and C. Hélène, *Angew. Chem., Int. Ed. Engl.*, 1993, **32**, 666.
4 L. Lavelle and J. Fresco, *Nucleic Acids Res.*, 1995, **23**, 2692.
5 F.-X. Barre, C. Glovannangeli, C. Hélène and A. Harel-Bellan, *Nucleic Acids Res.*, 1999, **27**, 743.
6 H. Okamura, Y. Taniguchi and S. Sasaki, *Angew. Chem., Int. Ed.*, 2016, **55**, 12445.
7 G. Gellert, M. N. Lipsett and D. R. Daveis, *Proc. Natl. Acad. Sci. U. S. A.*, 1962, **48**, 2013.
8 R. K. Moyzis, J. M. Buckingham, L. S. Cram, M. Dani, L. L. Deaven, M. D. Jones, J. Meyne, R. L. Ratliff and J.-R. Wu, *Proc. Natl. Acad. Sci. U. S. A.*, 1988, **85**, 6622.
9 C. M. Azzalin, P. Reichenback, L. Khoriauli, E. Giulotto and J. Linger, *Science*, 2007, **318**, 798.
10 Y. Wu, K. Kaminaga and M. Komiyama, *J. Am. Chem. Soc.*, 2008, **130**, 11179.
11 K. Gehring, J.-L. Leroy and M. Guéron, *Nature*, 1993, **363**, 561.
12 A. T. Phan and J.-L. Mergny, *Nucleic Acids Res.*, 2002, **30**, 4618.
13 P. A. Beal and P. B. Dervan, *Science*, 1991, **251**, 1360.
14 P. A. Beal and P. B. Dervan, *Nucleic Acids Res.*, 1992, **20**, 2773.
15 N. Avakyan, A. A. Greschner, F. Aldaye, C. J. Serpell, V. Toader, A. Petitjean and H. F. Sleiman, *Nat. Chem.*, 2016, **8**, 368.
16 P. E. Nielsen, M. Egholm, R. H. Berg and O. Buchardt, *Science*, 1991, **254**, 1497.
17 P. E. Nielsen, *Acc. Chem. Res.*, 1999, **32**, 624.
18 H. Kashida, K. Murayama, T. Toda and H. Asanuma, *Angew. Chem., Int. Ed.*, 2011, **50**, 1285.
19 H. Asanuma, T. Toda, K. Murayama, X. G. Liang and H. Kashida, *J. Am. Chem. Soc.*, 2010, **132**, 14702.
20 K. Murayama, H. Kashida and H. Asanuma, *Chem. Commun.*, 2015, **51**, 6500.
21 V. Kumar, V. Kesavan and K. V. Gothelf, *Org. Biomol. Chem.*, 2015, **13**, 2366.
22 Y. Kamiya, T. Satoh, A. Kodama, T. Suzuki, K. Murayama, H. Kashida, S. Uchiyama, K. Kato and H. Asanuma, *Commun. Chem.*, 2020, **3**, 156.
23 Y. Kamiya, F. Sato, K. Murayama, A. Kodama, S. Uchiyama and H. Asanuma, *Chem. – Asian J.*, 2020, **15**, 1266.
24 F. Sato, Y. Kamiya and H. Asanuma, *J. Org. Chem.*, 2023, **88**, 796.
25 V. Kumar and K. V. Gothelf, *Org. Biomol. Chem.*, 2016, **14**, 1540.
26 J. Meador, B. Cannnon, V. J. Cannistraro and D. Kennel, *Eur. J. Biochem.*, 1990, **187**, 549.
27 T. J. D. Nguyen, I. Manuguerra, V. Kumar and K. V. Gothelf, *Chem. – Eur. J.*, 2019, **25**, 12303.
28 H. B. Gamper, A. Gewirtz, J. Edwards and Y. M. Hou, *Biochemistry*, 2004, **43**, 10224.
29 J. Lohse, O. Dahl and P. E. Nielsen, *Proc. Natl. Acad. Sci. U. S. A.*, 1999, **96**, 11804.